

Article

The Effects of Running Kinematics on Peak Upper Trunk GPS-Measured Accelerations during Foot Contact at Different Running Speeds

Michael Lawson ^{1,2,*} , Roozbeh Naemi ^{1,*} , Robert A. Needham ¹ and Nachiappan Chockalingam ¹ 

¹ School of Health Science and Wellbeing, Staffordshire University, Stoke-on-Trent ST4 2DE, UK; r.needham@staffs.ac.uk (R.A.N.); n.chockalingam@staffs.ac.uk (N.C.)

² Middlesbrough Football Club, Middlesbrough TS3 6RS, UK

* Correspondence: michael.lawson@research.staffs.ac.uk (M.L.); r.naemi@staffs.ac.uk (R.N.)

Abstract: The overall aim of this study was to determine the effects of running kinematics on the peak upper trunk segmental accelerations captured with an accelerometer embedded in a commonly used GPS device. Thirteen male participants (age: 27 ± 3.7 years, height: 1.81 ± 0.06 m, mass: 82.7 ± 6.2 kg) with extensive running experience completed a single trial of treadmill running (1 degree inclination) for 40 s at nine different speeds ranging from 10 to 18 km/h at 1 km/h increments. Three-dimensional peak upper trunk acceleration values were captured via a GPS device containing a tri-axial accelerometer. Participants' running kinematics were calculated from the coordinate data captured by an 18-camera motion capture system. A series of generalized linear mixed models were employed to determine the effects of the kinematic variables on the accelerometer acceleration peaks across the key gait phases of foot contact. Results showed that running kinematics had significant effects on peak accelerometer-measured accelerations in all axes ($p < 0.05$). Overall, peak segment velocities had a larger effect than joint/segment kinematics on resultant (F values = 720.9/54.2), vertical (F values = 149.8/48.1) and medial–lateral (F values = 55.4/33.4) peak accelerometer accelerations. The largest effect on peak accelerometer accelerations were observed during the impact subphase of foot contact at the adduction/abduction velocity of the shank (F value = 129.2, coefficient = -0.03) and anterior/posterior velocity of the pelvis (F value = 58.9, coefficient = 0.01). Axis-dependent effects of running kinematics were also observed, specifically at the trunk segment in the vertical and anterior–posterior peak accelerometer accelerations. This study showed the intersegmental relationship between joint/segment kinematics, segment velocities and the resulting peak accelerations of the upper trunk during running over several speeds. These findings provide insights into the lower body's GRF attenuation capacity and its contribution to trunk stability whilst running.

Keywords: biomechanics; accelerometer/s; GPS; running; kinematics



Citation: Lawson, M.; Naemi, R.; Needham, R.A.; Chockalingam, N. The Effects of Running Kinematics on Peak Upper Trunk GPS-Measured Accelerations during Foot Contact at Different Running Speeds. *Appl. Sci.* **2024**, *14*, 63. <https://doi.org/10.3390/app14010063>

Academic Editor: Claudio Belvedere

Received: 6 November 2023

Revised: 16 December 2023

Accepted: 18 December 2023

Published: 20 December 2023



Copyright: © 2023 by the authors. Licensee MDPI, Basel, Switzerland. This article is an open access article distributed under the terms and conditions of the Creative Commons Attribution (CC BY) license (<https://creativecommons.org/licenses/by/4.0/>).

1. Introduction

Accelerometers are often employed in the field to analyze an athlete's running style as they are low cost, lightweight and have low power requirements [1]. Estimating joint angles is possible with multiple accelerometer setups by placing sensors on the relative segments above and/or below the joint [2–5]. However, they require extensive setup and data processing procedures to overcome errors associated with longitudinal analysis, such as sensor misalignment [6]. As a result, measuring the acceleration profile of a single segment and inferring changes in kinematics has often been a methodology employed in running-related studies that have analyzed a participant's running style over longer periods [7–11].

During foot contact, ground reaction forces are transmitted upwards through the kinetic chain, causing the individual segments to accelerate [12]. The accelerations and

subsequent velocities of each segment depend on the force transferred by the previous segment and the kinematic and anthropometric profiles of the segments [12]. Observing differences/changes in peak segmental accelerations has been previously employed within running-based studies to analyze the kinematic alterations within an individual's running style [10,13,14]. Suboptimal running kinematics can cause excessive soft tissue and bone stress during running, leading to injury [15] or reduced performance [16]. It is essential for sports science and medicine practitioners to ensure their athletes remain healthy and perform at a high level. Therefore, insights into an athlete's running kinematics will be beneficial to manage training load appropriately or to measure progress during an athlete's injury rehabilitation.

Employing a single accelerometer with minimal setup and data processing procedures to analyze running style is favorable when analyzing in the field with more than one athlete. Global positioning (GPS) devices are used with team sports athletes to monitor their training load by analyzing derivatives of distance and speed during training and match play [17]. These devices also contain an embedded tri-axial accelerometer, and most manufacturers' software calculates peak acceleration instances during a training session [18], offering a potentially convenient method to analyze an athlete's running style from already available data. When analyzing these peak accelerations, it is important to consider the mounting site of the accelerometer. The surrounding joints/segments of the segment to which the accelerometer is attached will influence the magnitude of the peak accelerations, and changes in running kinematics will alter the intersegmental transfer of force throughout the kinetic chain [14]. This has been previously shown at the shank, where peak accelerometer accelerations have increased when the position of the shank becomes more anteriorly rotated due to increased knee flexion [7]. The GPS devices, however, are positioned in a vest on the posterior aspect of the upper trunk. Therefore, the acceleration peaks captured by the accelerometer will potentially be influenced by the kinematics of the trunk, pelvis, thigh, shank and foot segments.

There has been a limited amount of research that has analyzed the effects of running kinematics on the acceleration profile of the trunk. Lindsay, Yaggie and McGregor (2014) investigated the contributions of the lower limb kinematics on the root mean square acceleration (overall magnitude of acceleration over the whole gait cycle) of an accelerometer placed on the lower trunk close to the center of mass. Sagittal plane kinematics of the hip, knee and ankle at initial foot contact, midstance and terminal foot contact were significantly correlated to the acceleration profile of the lower trunk [19]. Due to its size and anatomical structure, the trunk contains two segments: lower and upper [20]; the acceleration profiles of these two segments differ during running [21]. It has been previously suggested that the positioning of the GPS-based accelerometer device on the upper trunk was inappropriate for detecting changes in lower limb kinematics when analyzing the overall magnitude of acceleration during running due to noise caused within the acceleration profile by upper-limb movement [22]. However, the experimental setup in that study [22] did not allow for lower limb kinematics to be captured, so it remains unclear whether there is a relationship between running kinematics and the acceleration profile of the upper trunk. Furthermore, analyzing the peak acceleration of the upper trunk during foot contact, instead of the overall magnitude of acceleration, may provide a more sensitive measure to differences in running kinematics as utilized in other settings.

Naturally, there are inter-subject variations in running kinematics within a population of athletes. A simple method of inducing intra-subject changes is to alter the running speed [23,24]. As running speed increases, ground reaction forces and segment velocities increase and as a result, compensatory mechanisms of the musculoskeletal system are employed to attain stability of the trunk segments [25]. To gain a comprehensive insight into the intersegmental relationship between the lower body and trunk, analysis must be conducted over several different running speeds.

Therefore, this study aimed to determine the effects of running kinematics, over several speeds, on the peak upper trunk segmental accelerations during foot contact captured with

an accelerometer embedded in a commonly used GPS device by achieving the following objectives: (1) determine which joint/segments have the largest effect on the peak upper trunk accelerations at initial foot contact (IFC), midstance (MS) and terminal foot contact (TFC); (2) highlight the intersegmental relationship between segment velocities throughout the kinetic chain during foot contact by determining which segments influence the peak accelerations of the upper trunk.

Understanding which running kinematics have the greatest effect on the accelerometer data will allow sports science and medicine practitioners to use GPS-based accelerometer data to measure an athlete's running style in the field. We hypothesize that there will be a significant relationship between running kinematics and the peak accelerations captured by the GPS-embedded accelerometer.

2. Materials and Methods

2.1. Experimental Set Up

Thirteen male participants (age: 27 ± 3.7 years, height: 1.81 ± 0.06 m, mass: 82.7 ± 6.2 kg) with extensive running experience were recruited for this study. Participants completed a single trial of treadmill running (1 degree inclination) for 40 s at 9 different speeds starting at 10 km/h and proceeding to 18 km/h at 1 km/h increments. Maximum rest time was allowed between sets to ensure minimal fatigue accumulation. Participants were provided with standardized running shoes (Puma Anzarun) and wore an appropriately sized standard issue vest containing a GPS device (Statsports Apex, Northern Ireland, UK) which contained an embedded high-frequency tri-axial accelerometer. Each trial was captured by an 18-camera motion capture system (Vicon, Oxford, UK). Ethical clearance for this testing procedure was granted by the Staffordshire University Research Ethics Committee and all participants gave informed written consent prior to testing.

2.2. Data Processing

Eighteen optical cameras (VICON MXT40, Oxford, UK) recorded the coordinate data of fifty-four infrared markers (14 mm) attached to the participants at a frequency of 100 Hz. A modified Istituto Ortopedico Rizzoli (IOR) marker set with five additional clusters attached to the left thigh, right thigh, left shank, right shank and the posterior aspect of the GPS device [26–28] was employed to calculate kinematic variables. The global coordinate system defined the X-axis to represent anterior–posterior movement (positively oriented forward), the Y-axis for medio-lateral movement (positively oriented to the left), and the Z-axis for vertical movement (positively oriented upward). The coordinate data was then transferred from the Vicon Nexus software version-2.8.2 to Visual 3D (C-Motion Inc., Germantown, MD, USA) and filtered (4th order Butterworth, 10 Hz cut-off frequency).

The tri-axial accelerometer embedded within the GPS device was mounted around the posterior aspect of the thoracic spine (T2) and housed vertically within a standard issue vest. The orientation of the device aligned the Y-axis to vertical (VT) acceleration (positive in the upward direction), the X-axis to medio-lateral (ML) acceleration (positive in the left direction), and the Z-axis to anterior–posterior (AP) acceleration (positive in the forward direction). Time series data of the accelerometer was recorded at 100 Hz. Raw accelerometer data was transferred from the STATSports Apex software version-2.0 to Visual 3D software version-2022 (C-Motion Inc., Germantown, MD, USA).

To synchronize the data between the optical motion capture system and accelerometer, an assistant 'tapped' the GPS device in a downward vertical direction at the beginning of each trial. The frame of the tap was identified in both data sets. Ten consecutive gait cycles were selected for analysis following a 20 s ramp period to allow for participants to reach the target running speed.

2.3. Running Kinematic Variables

A total of 160 kinematics variables were calculated during key gait events of foot stance to provide a comprehensive insight into the intersegmental relationship between

joint/segment angles and subsequent segment velocities throughout the stance phase. A kinematic method [29,30] was employed to determine IFC, MS and TFC. Three-dimensional joint/segment angles were calculated for the thorax, trunk, pelvis, hip, thigh, knee, shank, ankle and foot at IFC, MS and TFC. Additionally, three-dimensional peak segment velocities were calculated for the thorax, trunk, pelvis, thigh, shank and foot during the two subphases of foot stance (IFC–MS and MS–TFC). Averages of each variable were calculated across the ten gait cycles.

2.4. Accelerometer Variables

Peak accelerometer accelerations during foot stance were calculated by initially identifying the time events of IFC and TFC within the accelerometer data (as per the authors' prior study). Within each instance of foot stance, the peak acceleration values for each axis and resultant (RES) acceleration were identified. The averages of the peak acceleration values were calculated across the ten cycles for each axis and resultant acceleration.

2.5. Statistical Analysis

Generalized linear mixed model (GLMM) analysis was selected as the appropriate method of establishing the effects of the running kinematics (fixed effects) on peak accelerometer accelerations (dependent variables) due to the study design containing multiple measures per subject. GLMMs are regression models that allow for autocorrelation and are therefore preferred when observations are not independent and contain repeated measures [31,32]. The data structure of the fixed effect and dependent variables were continuous, so a linear model with identity link function $f(x) = x$ was employed.

A series of GLMMs were conducted due to the number of fixed effect and dependent variables. Fixed effect variables were separated into two categories, and the running speed was defined as the repeated measure. Category 1 contained the joint/segment three-dimensional kinematics at IFC, MS and TFC. Category 2 contained the peak segmental velocities between IFC–MS and MS–TFC. Preliminary GLMM analysis was conducted on the individual joint/segment kinematics, separately for category 1 and 2 variables against each dependent variable, to filter out non-significant variables (p value > 0.05).

The remaining category 1 and 2 fixed effect variables were then further analyzed by GLMM against each dependent variable. A type III F-test was used to determine the magnitude of the effect of each fixed effect variable (F value), whether it was direct or inverse (fixed effect coefficient) and if it was significant (p value < 0.05). Averages and standard deviations of all F values were calculated to separate the significant fixed effect variables into groups of small effect: F value $<$ average $- (0.5 * \text{standard deviation})$; medium effect: F value $>$ average $- (0.5 * \text{standard deviation})$ and $<$ average $+ (0.5 * \text{standard deviation})$; large effect: F value $>$ average $+ (0.5 * \text{standard deviation})$. Mean difference (g) between the actual and predicted peak accelerometer accelerations with 95% limits of agreement (LOA) were also calculated from the GLMMs to assess accuracy of each model. In addition, residual effect estimates were calculated to understand the residual effect of running speed on the GLMMs. Statistical analysis was conducted using SPSS software version-29.0.0.0 (IBM Corporation, Armonk, NY, USA).

3. Results

GLMMs for category 1 and 2 fixed effect variables showed a significant relationship for all dependent variables ($p < 0.05$, Table 1). Model summaries of the category 1 fixed effect GLMMs to estimate the peak accelerations were RES (mean difference: -0.01 g; LOA: -0.43 g, 0.42 g; F value: 54.18; $p < 0.05$), VT (mean difference: -0.01 g; LOA: -0.49 g, 0.47 g; F value: 48.06; $p < 0.05$), AP (mean difference: 0.00 g; LOA: -0.16 g, 0.17 g; F value: 56.43; $p < 0.05$) and ML (mean difference: -0.01 g; LOA: -0.20 g, 0.18 g; F value: 33.41; $p < 0.05$). Model summaries of the category 2 fixed effect GLMMs to estimate the peak accelerations were RES (mean difference: 0.00 g; LOA: -0.42 g, 0.43 g; F value: 720.83; $p < 0.05$), VT (mean difference: -0.01 g; LOA: -0.61 g, 0.64 g; F value: 149.79; $p < 0.05$),

AP (mean difference: 0.00 g; LOA: -0.21 g, 0.21 g; F value: 53.93; $p < 0.05$) and ML (mean difference: 0.00 g; LOA: -0.17 g, 0.17 g; F value: 55.38; $p < 0.05$). Significant residual effects of running speed were observed on peak RES, VT and ML accelerations for category 1 fixed effect variables ($p < 0.05$, Table 2). However, running speed had significant residual effects on all peak accelerations for category 2 fixed effect variables ($p < 0.05$, Table 3).

Table 1. GLMM summary of category 1 and 2 fixed effect variables for each dependent variable.

GLMM	Peak RES Acceleration		Peak VT Acceleration		Peak AP Acceleration		Peak ML Acceleration	
	F Value	Significance	F Value	Significance	F Value	Significance	F Value	Significance
Category 1	54.18	0.00 *	48.07	0.00 *	56.43	0.00 *	33.41	0.00 *
Category 2	720.89	0.00 *	149.79	0.00 *	53.92	0.00 *	55.38	0.00 *

* Significance is <0.05

Table 2. The residual effect of running speed on peak accelerations of the GPS-embedded accelerometer for category 1 fixed effect variables.

Speed	Peak RES Acceleration		Peak VT Acceleration		Peak AP Acceleration		Peak ML Acceleration	
	Estimate	Significance	Estimate	Significance	Estimate	Significance	Estimate	Significance
10 km/h	0.08	0.04 *	0.12	0.04 *	0.01	0.14	0.01	0.10
11 km/h	0.03	0.10	0.03	0.17	0.01	0.28	0.02	0.04 *
12 km/h	0.08	0.03 *	0.08	0.04 *	0.01	0.10	0.01	0.08
13 km/h	0.04	0.09	0.04	0.20	0.03	0.11	0.01	0.10
14 km/h	0.01	0.22	0.04	0.13	0.01	0.10	0.01	0.06
15 km/h	0.04	0.12	0.04	0.16	0.00	0.45	0.00	0.40
16 km/h	0.04	0.10	0.09	0.09	0.01	0.20	0.01	0.09
17 km/h	0.09	0.05	0.07	0.09	0.01	0.28	0.00	0.52
18 km/h	0.11	0.06	0.11	0.06	0.01	0.20	0.04	0.04 *

* Significance is <0.05 .

Table 3. The residual effect of running speed on peak accelerations of the GPS-embedded accelerometer for category 2 fixed effect variables.

Speed	Peak RES Acceleration		Peak VT Acceleration		Peak AP Acceleration		Peak ML Acceleration	
	Estimate	Significance	Estimate	Significance	Estimate	Significance	Estimate	Significance
10 km/h	0.09	0.04 *	0.12	0.02 *	0.02	0.07	0.00	0.21
11 km/h	0.06	0.04 *	0.00	0.82	0.01	0.07	0.01	0.02 *
12 km/h	0.02	0.16	0.05	0.07	0.01	0.04 *	0.00	0.19
13 km/h	0.19	0.03 *	0.18	0.04 *	0.02	0.07	0.00	0.20
14 km/h	0.01	0.23	0.05	0.08	0.01	0.07	0.01	0.04 *
15 km/h	0.01	0.26	0.16	0.05	0.01	0.08	0.01	0.06
16 km/h	0.05	0.14	0.14	0.10	0.02	0.09	0.01	0.04 *
17 km/h	0.09	0.06	0.16	0.05	0.02	0.14	0.01	0.06
18 km/h	0.10	0.06	0.28	0.12	0.01	0.25	0.03	0.05

* Significance is <0.05 .

F-test results showed significant effects ($p < 0.05$) of category 1 fixed effect variables on the peak accelerations in the upper-trunk-mounted accelerometer, which varied between axes and were dependent on the phase during contact. For peak RES accelerations, the thorax (IFC), pelvis (MS), hip (IFC and MS), knee (IFC and TFC), shank (TFC) and ankle (MS) had significant ($p < 0.05$) F values ranging from 5.4 to 26.4 (Figure 1). For peak VT accelerations, the thorax (IFC and TFC), pelvis (IFC, MS and TFC), hip (IFC), knee (TFC) and ankle (MS) had significant ($p < 0.05$) F values ranging from 4.2 to 18.2 (Figure 2). For peak AP accelerations, the thorax (MS), pelvis (IFC), ankle (MS), and foot (TFC) had significant ($p < 0.05$) F values ranging from 4.3 to 10.9 (Figure 3). Lastly, for peak ML accelerations, the

thorax (MS), pelvis (IFC), ankle (MS) and foot (TFC) all had significant ($p < 0.05$) F values ranging from 4.2 to 5.3 (Figure 4).

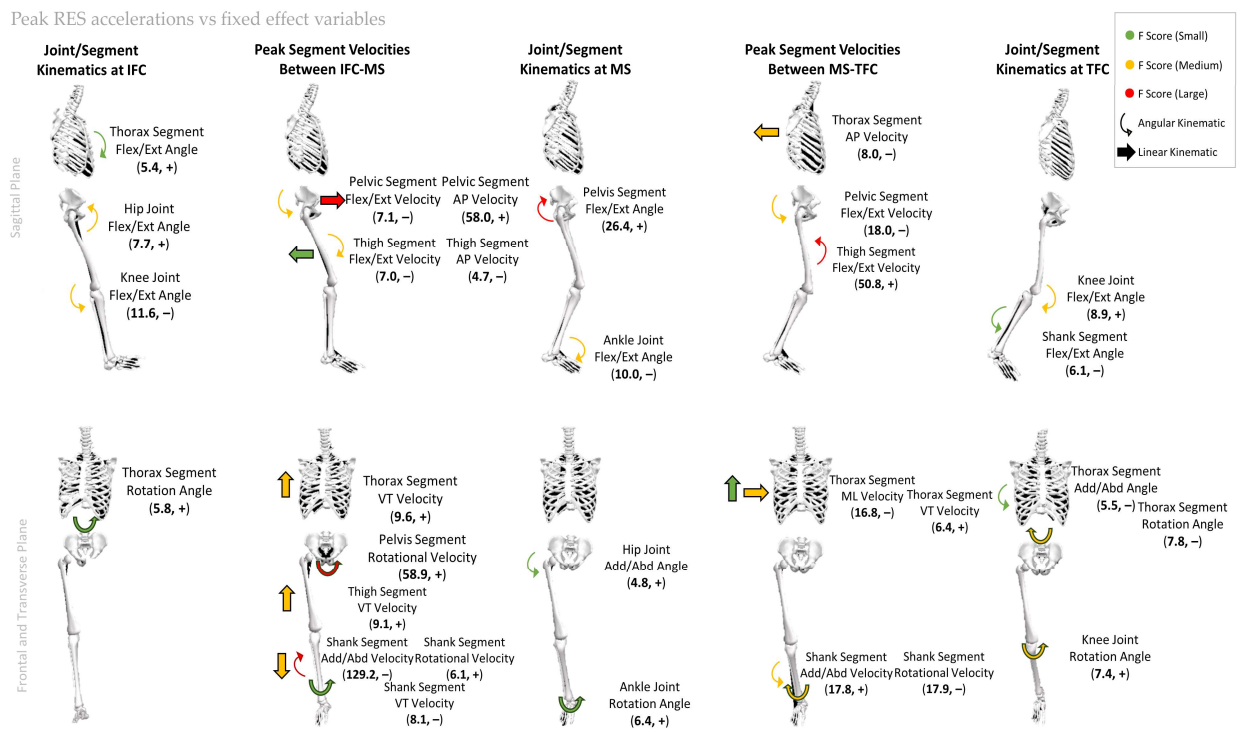


Figure 1. Category 1 and 2 variables with a significant effect ($p < 0.05$) on the peak RES accelerations of the GPS-based accelerometer at each key gait phase. F value and fixed effect coefficient (+ = direct, - = inverse) are displayed within the brackets of each variable. The direction of the arrows represents the motion of the joint/segment that has a significant effect at each key gait phase.

Peak VT accelerations vs fixed effect variables

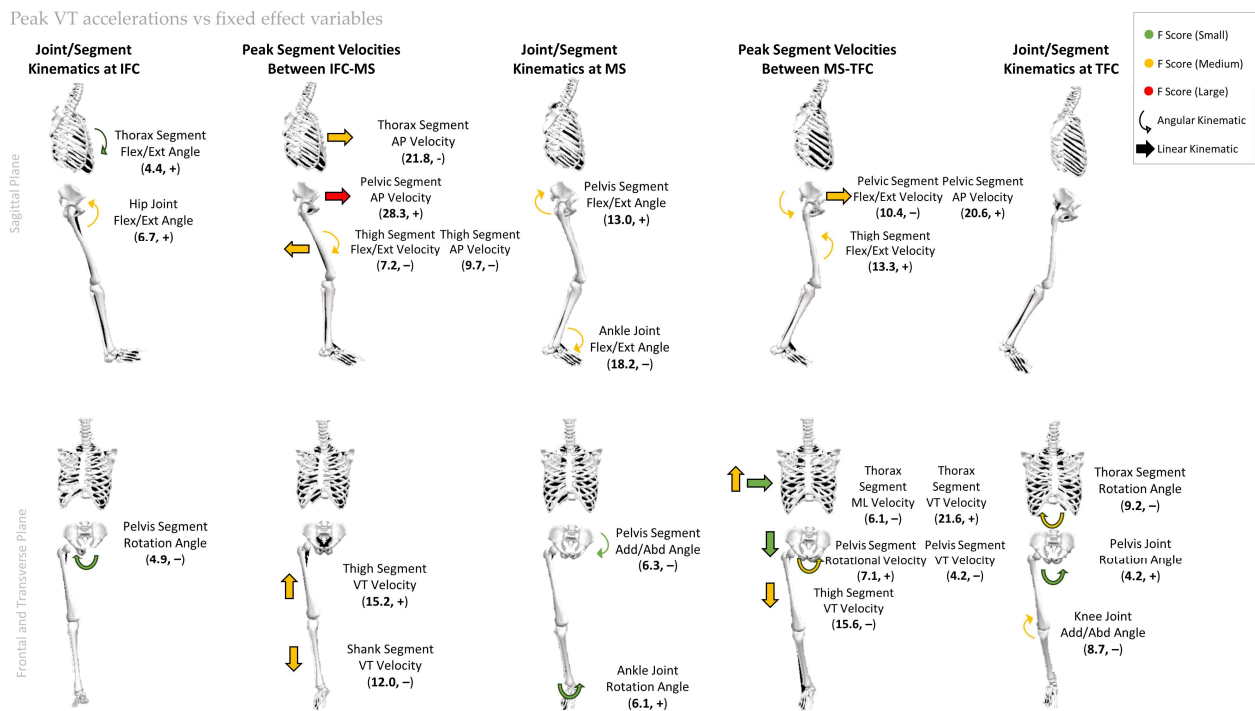


Figure 2. Category 1 and 2 variables with a significant effect ($p < 0.05$) on the peak VT accelerations of the GPS-based accelerometer at each key gait phase. F value and fixed effect coefficient (+ = direct, - = inverse) are displayed within the brackets of each variable. The direction of the arrows represents the motion of the joint/segment that has a significant effect at each key gait phase.

Peak AP accelerations vs fixed effect variables

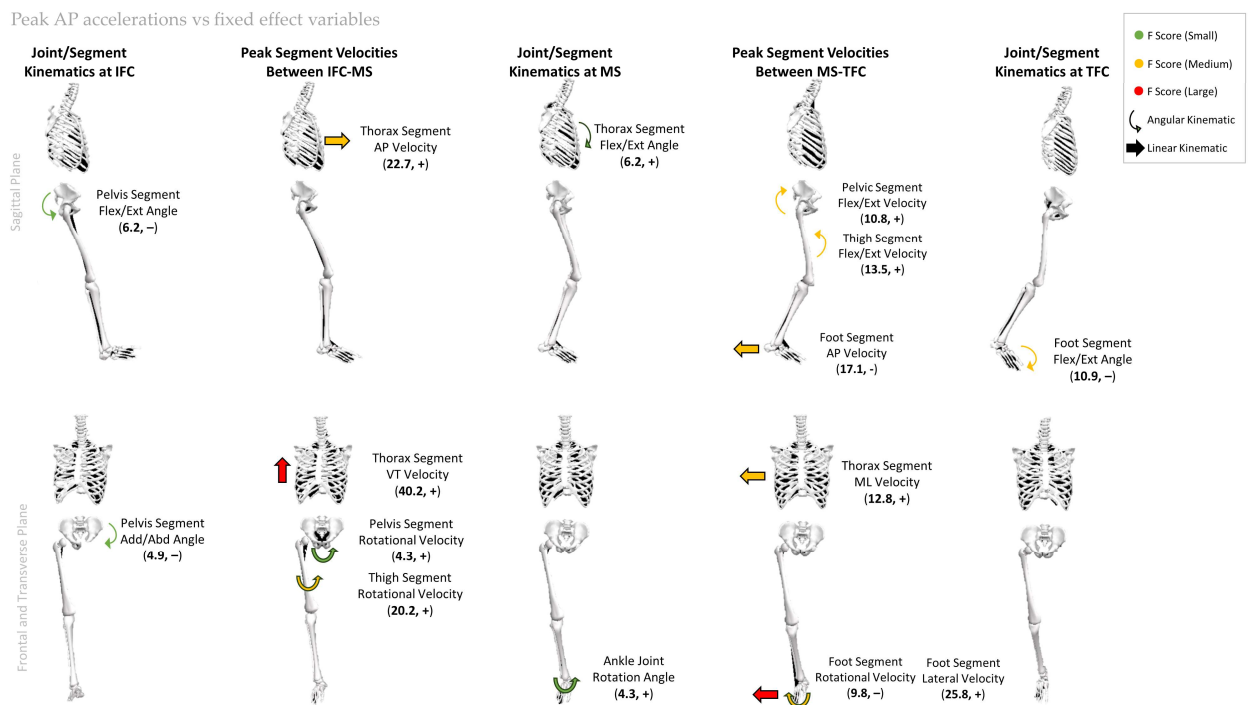


Figure 3. Category 1 and 2 variables with a significant effect ($p < 0.05$) on the peak AP accelerations of the GPS-based accelerometer at each key gait phase. F value and fixed effect coefficient (+ = direct, - = inverse) are displayed within the brackets of each variable. The direction of the arrows represents the motion of the joint/segment that has a significant effect at each key gait phase.

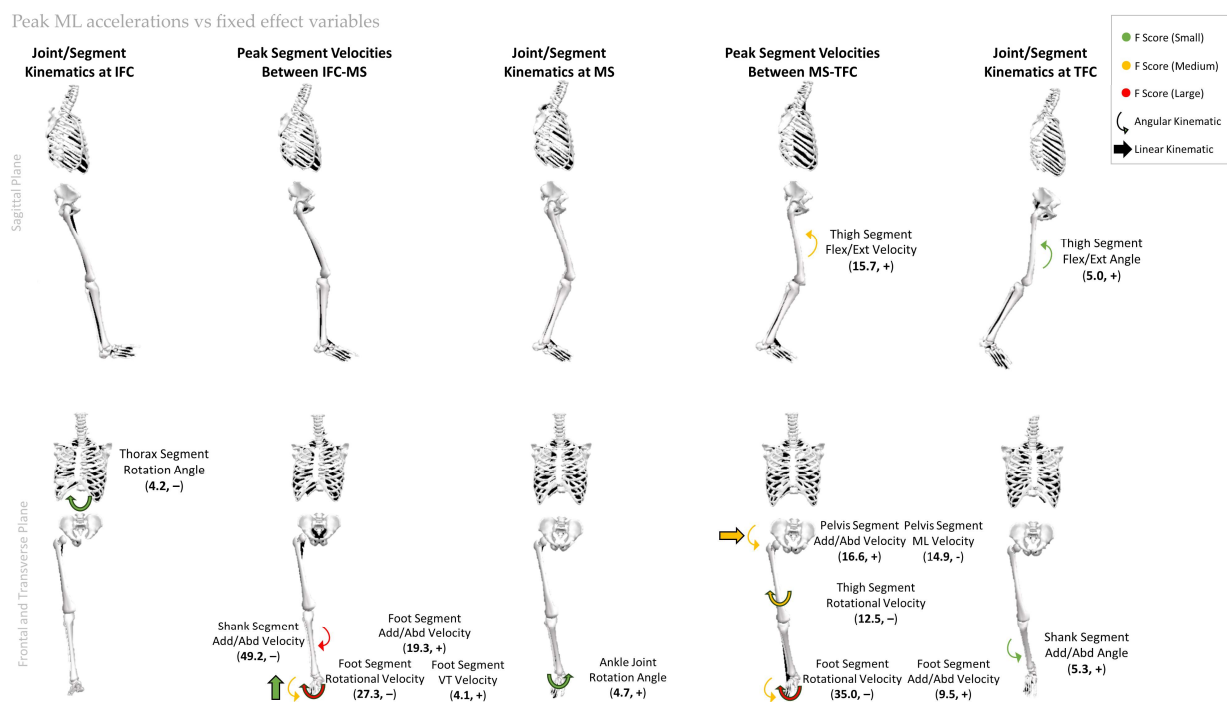


Figure 4. Category 1 and 2 variables with a significant effect ($p < 0.05$) on the peak ML accelerations of the GPS-based accelerometer at each key gait phase. F value and fixed effect coefficient (+ = direct, − = inverse) are displayed within the brackets of each variable. The direction of the arrows represents the motion of the joint/segment that has a significant effect at each key gait phase.

Category 2 fixed effect variables had significant effects in both subphases of foot contact (IFC–MS and MS–TFC) and the largest range in F values (4.2–129.2). For RES, VT and AP peak accelerations, the thorax, pelvis and thigh significantly affected both subphases ($p < 0.05$, Figures 1–3). The shank had a significant effect in both subphases for RES but only in IFC–MS for VT and ML acceleration peaks ($p < 0.05$, Figures 1, 2 and 4). The foot also had a significant effect in AP during MS–TFC and during both subphases for ML acceleration peaks ($p < 0.05$, Figures 3 and 4). In addition, the pelvis and thigh significantly affected ML acceleration peak during MS–TFC ($p < 0.05$, Figure 4).

The reader is encouraged to take notice of the coefficients (+/−) in Figures 1–4 to understand whether the effects of the kinematics were direct or inverse. In addition, the entire F-test results from the GLMMs can be found in the Supplementary Materials (Tables S1–S12).

4. Discussion

The present study aimed to determine the effects of running kinematics during foot contact on the peak upper trunk accelerations captured by an accelerometer embedded within a commonly used GPS tracking device. Variables of running kinematics were separated into two categories: joint/segment kinematics at IFC, MS and TFC, and peak segment velocities between IFC–MS and MS–TFC. Analyzing these variables independently, through GLMMs, allowed for insights into which joint/segments have the largest effect on the peak upper trunk accelerations, during which key gait event this occurs and the effect of the subsequent peak velocities of the bodily segments during the impact (IFC–MS) and propulsion (MS–TFC) subphases of foot contact.

GLMM summaries showed that category 2 fixed effect variables (peak segment velocities) had a larger effect (F value) than the category 1 fixed effect variables (joint/segment kinematics) on the RES, VT and ML accelerometer peak accelerations (Table 1). In addition, running speed had a greater residual effect on the category 2 fixed variables (Table 2). To our knowledge, these comparisons have not been previously reported; however, they

substantiate the relationships described by Derrick (2004) on the determinants of bodily segmental accelerations when exposed to impact forces during running. These findings infer that including segment velocities in future studies can lead to a better understanding of the intersegmental relationship during running instead of focusing on joint kinematics alone, as seen in previous studies [7,19,33].

It has previously been well documented that increased joint stiffness and stability around the lower limb segments result in less GRF attenuation and more force transferring up the kinetic chain, leading to greater impact and propulsion forces during running [19,34,35]. Our results support findings from Lindsay et al. (2014) as decreased knee flexion at IFC increases the shank segment's stability, reducing the shank's peak linear and angular velocities during the impact subphase (IFC–MS) and causing greater peak accelerometer accelerations (Figure 1). The shank segment had the largest effect on peak RES (F value = 129.2, Figure 1) and ML (F value = 49.2, Figure 4) accelerometer accelerations of all peak segment velocities, thus displaying its important role in the transfer of GRF throughout the kinetic chain.

Additionally, during MS, the role of the ankle is apparent as there is a medium-sized effect of decreased ankle flexion resulting in larger RES (F value = 10.0, Figure 1) and VT (F value = 18.2, Figure 2) peak accelerations, suggesting that larger acceleration peaks are related to reduced decoupling of the ankle joint. Increased joint stiffness can increase propulsion forces capabilities during stance [35], resulting in larger peak segment velocities. This is shown in the propulsion subphase (MS–TFC) as increased peak angular (flexion) velocity of the thigh has a large to medium-sized effect on the peak accelerometer accelerations in all axes (Figures 1–4). Furthermore, large to medium-sized effects were observed for foot segment linear (posterior and medial) and angular (internal rotation) peak velocities on the AP and ML peak accelerometer accelerations (Figures 3 and 4). These findings differ from previous investigations [19] as the ankle flexion angle was associated with TFC and they did not analyze segmental velocities, possibly due to the different accelerometer mounting sites.

The proximal joints and segments of the trunk were shown in our results also to influence the peak accelerometer accelerations. During impact (IFC–MS), the second largest effect on peak RES accelerometer accelerations was observed at the pelvis segment (F value = 58.0, Figure 1). Increased hip flexion at IFC, which also supports previous findings [19], reduces the effective mass of the pelvis segment [12], causing increased linear (anterior) and angular (internal rotation) peak velocities during impact (IFC–MS) (Figure 1). This results in increased flexion of the pelvis at MS due to the pelvis decoupling to support the deceleration of the trunk segment post-impact as it supports trunk stability. During propulsion (MS–TFC), there are medium-sized effects of pelvis angular (extension and internal rotation) and linear (anterior) peak velocities, which contribute to larger RES and VT peak accelerometer accelerations (Figures 1 and 2). Conversely, reduced extension peak velocities (increased flexion) at the pelvis contributed to larger AP peak accelerometer accelerations, and greater frontal plane peak velocities at the pelvis resulted in larger ML peak accelerometer accelerations (Figures 3 and 4). This indicates that insights can be gained into pelvis extension and stability properties of athletes by analyzing the differences between VT, AP and ML peak accelerometer accelerations.

Furthermore, similar differences between the peak accelerometer accelerations were also observed regarding the thorax segment velocities. Reduced peak linear (anterior) velocity during impact and increased peak linear (vertical) velocity during propulsion of the thorax resulted in larger VT peak accelerometer accelerations (Figure 2). Whereas increased linear (vertical and anterior) peak velocity during impact and increased linear (lateral) peak velocity during propulsion of the thorax resulted in larger AP peak accelerometer accelerations (Figure 3). As force is transferred from the pelvis to the trunk, the surrounding musculature is activated to maintain stability and influences the subsequent displacement of the trunk segment [25]. Therefore, our results suggest that analyzing the

differences between the VT and AP peak accelerometer accelerations may provide insights into these mechanisms.

Findings from this study show that GRF attenuation properties of the surrounding joints to the shank segment and the kinematics of the pelvis in maintaining trunk stability, specifically at MS, have the largest effects on the peak accelerometer accelerations. Practical applications of these findings are that peak accelerometer accelerations could be valuable in analyzing an athlete's rehabilitation from an ACL reconstruction, as this has been shown to affect knee extension during running [36]. Alternatively, observing the differences between the axis of peak accelerometer accelerations throughout an athlete's training session may be used to provide insight into the level of neuromuscular fatigue affecting the stability of pelvis/trunk segments [37,38].

While a direct comparison of our results to those of Lindsey et al. (2014) was not possible due to the differences in statistical analysis between the studies, similar findings were observed regarding the significant effects of the hip and knee flexion/extension angle on the RES acceleration profile at IFC (Figure 1).

The present study utilized GLMMs as repeated measures were present, whereas Lindsey et al. (2014) employed a stepwise regression analysis. Lindsey et al. (2014) mounted their accelerometer on the lower trunk. Therefore, it can be suggested that hip and knee kinematics at IFC affect both the lower and upper trunk acceleration profiles.

In addition, our results refute previous suggestions [22] that the mounting site of the accelerometer on the upper trunk is unacceptable for observing changes in lower limb running kinematics. The limitations of the present study are that the findings only apply to straight-line running, as the trials were conducted on a treadmill. It is suggested that practitioners utilize the coordinate data from the GPS devices to ensure instances of straight-line running are selected when applying the current findings to field-based running style analysis [39]. Treadmill running was selected in the study design to control the running speed and to induce intra-subject variations in running kinematics by altering the speed between each trial. As a result, ground reaction forces were not captured due to the absence of an embedded force platform. Considering the residual effects of the running speed observed, especially in the category 2 fixed effect variables, understanding the associated changes in joint/segment kinetics with each running speed and how they differed across a wider variety of running styles would have provided a more comprehensive insight into the effect of different running styles on the GPS-based accelerometer accelerations. The outcome of this study was favorable, considering the significant associations found with relatively small participants. In the future, having a bigger sample size would allow for further verifications of the outcome of this study.

5. Conclusions

In summary, GLMMs within this study have demonstrated the intersegmental relationship between joint/segment kinematics, segment velocities and the resulting peak accelerations of the upper trunk during running over several speeds. Specifically, we found that peak shank and pelvis velocities during impact (IFC-MS) had the largest effect on the RES upper trunk peak accelerations captured by the accelerometer contained within the GPS device. Furthermore, differences in pelvis and thorax peak velocities affected the peak accelerometer accelerations in the individual axes (VT, AP and ML). Sports science and medical practitioners may utilize analysis of peak RES GPS-based accelerometer accelerations to provide insights into the lower body's GRF attenuation properties during impact. Additionally, analyzing the differences between the peak accelerometer accelerations in each axis can infer an athlete's trunk stability mechanisms whilst running. The findings of this study provide the basis for analyzing an athlete's running style in the field with the peak accelerations captured from the GPS-based accelerometer. Information of this kind could be used to monitor an athlete's progress during injury rehabilitation and training load management.

Supplementary Materials: The following supporting information can be downloaded at <https://www.mdpi.com/article/10.3390/app14010063/s1>: Table S1. Category 1 Peak RES Accelerations GLMM results; Table S2. Category 1 Peak VT Accelerations GLMM results; Table S3. Category 1 Peak AP Accelerations GLMM results; Table S4. Category 1 Peak ML Accelerations GLMM results; Table S5. Category 2 Peak RES Accelerations GLMM results; Table S6. Category 2 Peak VT Accelerations GLMM results; Table S7. Category 2 Peak AP Accelerations GLMM results; Table S8. Category 2 Peak ML Accelerations GLMM results; Table S9. Actual Peak RES Accelerations vs. GLMM predicted for Category 1 and 2 variables; Table S10. Actual Peak VT Accelerations vs. GLMM predicted for Category 1 and 2 variables; Table S11. Actual Peak AP Accelerations vs. GLMM predicted for Category 1 and 2 variables; Table S12. Actual Peak ML Accelerations vs. GLMM predicted for Category 1 and 2 variables.

Author Contributions: M.L. was the principal researcher on this study. The contributions by the authors are as follows: Conceptualization, M.L., R.A.N., R.N. and N.C.; Methodology, M.L. and R.N.; Software, M.L. and R.A.N.; Formal Analysis, M.L., R.N. and R.A.N.; Writing—Original Draft Preparation, M.L. and R.N.; Writing—Reviewing and Editing, R.A.N., R.N. and N.C.; Visualization, M.L.; Supervision, R.N. and N.C. All authors have read and agreed to the published version of the manuscript.

Funding: This research received no external funding.

Institutional Review Board Statement: Ethical clearance for this testing procedure was granted by the Staffordshire University ethical committee (9 October 2019).

Informed Consent Statement: All participants gave informed written consent prior to testing.

Data Availability Statement: The data presented in this study are available in the main text (Tables 1–3) and in the Supplementary Materials (Tables S1–S12).

Conflicts of Interest: The authors can declare that there are no conflicts of interest regarding the publication of this study.

References

1. Cronin, N.J. Using Deep Neural Networks for Kinematic Analysis: Challenges and Opportunities. *J. Biomech.* **2021**, *123*, 110460. [[CrossRef](#)] [[PubMed](#)]
2. Mihcin, S. Simultaneous Validation of Wearable Motion Capture System for Lower Body Applications: Over Single Plane Range of Motion (ROM) and Gait Activities. *Biomed. Eng. Biomed. Technol.* **2022**, *67*, 185–199. [[CrossRef](#)] [[PubMed](#)]
3. Stetter, B.J.; Krafft, F.C.; Ringhof, S.; Stein, T.; Sell, S. A Machine Learning and Wearable Sensor Based Approach to Estimate External Knee Flexion and Adduction Moments during Various Locomotion Tasks. *Front. Bioeng. Biotechnol.* **2020**, *8*, 9. [[CrossRef](#)] [[PubMed](#)]
4. Dorschky, E.; Nitschke, M.; Martindale, C.F.; van den Bogert, A.J.; Koelewijn, A.D.; Eskofier, B.M. CNN-Based Estimation of Sagittal Plane Walking and Running Biomechanics from Measured and Simulated Inertial Sensor Data. *Front. Bioeng. Biotechnol.* **2020**, *8*, 604. [[CrossRef](#)] [[PubMed](#)]
5. Gholami, M.; Rezaei, A.; Cuthbert, T.J.; Napier, C.; Menon, C. Lower Body Kinematics Monitoring in Running Using Fabric-Based Wearable Sensors and Deep Convolutional Neural Networks. *Sensors* **2019**, *19*, 5325. [[CrossRef](#)] [[PubMed](#)]
6. Zimmermann, T.; Taetz, B.; Bleser, G. IMU-to-Segment Assignment and Orientation Alignment for the Lower Body Using Deep Learning. *Sensors* **2018**, *18*, 302. [[CrossRef](#)] [[PubMed](#)]
7. Mizrahi, J.; Verbitsky, O.; Isakov, E.; Daily, D. Effect of Fatigue on Leg Kinematics and Impact Acceleration in Long Distance Running. *Hum. Mov. Sci.* **2000**, *19*, 139–151. [[CrossRef](#)]
8. Ruder, M.; Jamison, S.T.; Tenforde, A.; Mulloy, F.; Davis, I.S. Relationship of Foot Strike Pattern and Landing Impacts during a Marathon. *Med. Sci. Sports Exerc.* **2019**, *51*, 2073–2079. [[CrossRef](#)]
9. Johnson, C.D.; Outerleys, J.; Jamison, S.T.; Tenforde, A.S.; Ruder, M.; Davis, I.S. Comparison of Tibial Shock during Treadmill and Real-World Running. *Med. Sci. Sports Exerc.* **2020**, *52*, 1557–1562. [[CrossRef](#)]
10. Abt, J.J.P.; Sell, T.T.C.; Chu, Y.; Lovalekar, M.; Burdett, R.G.; Lephart, S.M. Running Kinematics and Shock Absorption Do Not Change after Brief Exhaustive Running. *J. Strength Cond. Res.* **2011**, *25*, 1479–1485. [[CrossRef](#)]
11. Blackah, N.; Bradshaw, E.J.; Kemp, J.G.; Shoushtarian, M. The Effect of Exercise-Induced Muscle Damage on Shock Dissipation during Treadmill Running. *Asian J. Exerc. Sports Sci.* **2013**, *10*, 16–30.
12. Derrick, T.R. The Effects of Knee Contact Angle on Impact Forces and Accelerations. *Med. Sci. Sports Exerc.* **2004**, *36*, 832–837. [[CrossRef](#)] [[PubMed](#)]
13. Garcia, M.C.; Gust, G.; Bazett-Jones, D.M. Tibial Acceleration and Shock Attenuation While Running over Different Surfaces in a Trail Environment. *J. Sci. Med. Sport* **2021**, *24*, 1161–1165. [[CrossRef](#)] [[PubMed](#)]

14. Hamill, J.; Derrick, T.R.; Holt, K.G. Shock Attenuation and Stride Frequency during Running. *Hum. Mov. Sci.* **1995**, *14*, 45–60. [[CrossRef](#)]
15. Hesar, N.G.Z.; Van Ginckel, A.; Cools, A.; Peersman, W.; Roosen, P.; De Clercq, D.; Witvrouw, E. A Prospective Study on Gait-Related Intrinsic Risk Factors for Lower Leg Overuse Injuries. *Br. J. Sports Med.* **2009**, *43*, 1057–1061. [[CrossRef](#)] [[PubMed](#)]
16. Folland, J.P.; Allen, S.J.; Black, M.I.; Handsaker, J.C.; Forrester, S.E. Running Technique Is an Important Component of Running Economy and Performance. *Med. Sci. Sports Exerc.* **2017**, *49*, 1412–1423. [[CrossRef](#)] [[PubMed](#)]
17. Buchheit, M.; Gray, A.; Morin, J.-B.B. Assessing Stride Variables and Vertical Stiffness with GPS-Embedded Accelerometers: Preliminary Insights for the Monitoring of Neuromuscular Fatigue on the Field. *J. Sports Sci. Med.* **2015**, *14*, 698–701.
18. Wundersitz, D.W.T.; Gastin, P.B.; Robertson, S.; Davey, P.C.; Netto, K.J. Validation of a Trunk-Mounted Accelerometer to Measure Peak Impacts during Team Sport Movements. *Int. J. Sports Med.* **2015**, *36*, 742–746. [[CrossRef](#)]
19. Lindsay, T.R.; Yaggie, J.A.; McGregor, S.J. Contributions of Lower Extremity Kinematics to Trunk Accelerations during Moderate Treadmill Running. *J. Neuroeng. Rehabil.* **2014**, *11*, 162. [[CrossRef](#)]
20. Drillis, R.; Contini, R.; Bluestein, M. Body Segment Parameters; a Survey of Measurement Techniques. *Artif. Limbs* **1964**, *25*, 44–66. [[CrossRef](#)]
21. Kawabata, M.; Goto, K.; Fukusaki, C.; Sasaki, K.; Hihara, E.; Mizushina, T.; Ishii, N. Acceleration Patterns in the Lower and Upper Trunk during Running. *J. Sports Sci.* **2013**, *31*, 1841–1853. [[CrossRef](#)] [[PubMed](#)]
22. Barrett, S.; Midgley, A.; Lovell, R. PlayerLoadTM: Reliability, Convergent Validity, and Influence of Unit Position during Treadmill Running. *Int. J. Sports Physiol. Perform.* **2014**, *9*, 945–952. [[CrossRef](#)] [[PubMed](#)]
23. Fukuchi, R.K.; Fukuchi, C.A.; Duarte, M. A Public Dataset of Running Biomechanics and the Effects of Running Speed on Lower Extremity Kinematics and Kinetics. *PeerJ* **2017**, *5*, e3298. [[CrossRef](#)] [[PubMed](#)]
24. Brughelli, M.; Cronin, J.; Chaouachi, A. Effects of Running Velocity on Running Kinetics and Kinematics. *J. Strength Cond. Res.* **2011**, *25*, 933–939. [[CrossRef](#)] [[PubMed](#)]
25. Saunders, S.W.; Schache, A.; Rath, D.; Hodges, P.W. Changes in Three Dimensional Lumbo-Pelvic Kinematics and Trunk Muscle Activity with Speed and Mode of Locomotion. *Clin. Biomech.* **2005**, *20*, 784–793. [[CrossRef](#)] [[PubMed](#)]
26. Leardini, A.; Sawacha, Z.; Paolini, G.; Ingrosso, S.; Nativio, R.; Benedetti, M.G. A New Anatomically Based Protocol for Gait Analysis in Children. *Gait Posture* **2007**, *26*, 560–571. [[CrossRef](#)] [[PubMed](#)]
27. Leardini, A.; Biagi, F.; Merlo, A.; Belvedere, C.; Benedetti, M.G. Multi-Segment Trunk Kinematics during Locomotion and Elementary Exercises. *Clin. Biomech.* **2011**, *26*, 562–571. [[CrossRef](#)]
28. Needham, R.; Naemi, R.; Healy, A.; Chockalingam, N. Multi-Segment Kinematic Model to Assess Three-Dimensional Movement of the Spine and Back during Gait. *Prosthet. Orthot. Int.* **2016**, *40*, 624–635. [[CrossRef](#)]
29. Lee, J.B.; Mellifont, R.B.; Burkett, B.J. The Use of a Single Inertial Sensor to Identify Stride, Step, and Stance Durations of Running Gait. *J. Sci. Med. Sport* **2010**, *13*, 270–273. [[CrossRef](#)]
30. Lussiana, T.; Gindre, C.; Mourot, L.; Hébert-Losier, K. Do Subjective Assessments of Running Patterns Reflect Objective Parameters? *Eur. J. Sport Sci.* **2017**, *17*, 847–857. [[CrossRef](#)]
31. Bono, R.; Alarcón, R.; Blanca, M.J. Report Quality of Generalized Linear Mixed Models in Psychology: A Systematic Review. *Front. Psychol.* **2021**, *12*, 666182. [[CrossRef](#)] [[PubMed](#)]
32. Thiele, J.; Markussen, B. Potential of GLMM in Modelling Invasive Spread. *CABI Rev.* **2012**, *7*, 1–10. [[CrossRef](#)]
33. Quan, W.; Zhou, H.; Xu, D.; Li, S.; Baker, J.S.; Gu, Y. Competitive and Recreational Running Kinematics Examined Using Principal Components Analysis. *Healthcare* **2021**, *9*, 1321. [[CrossRef](#)] [[PubMed](#)]
34. Hennig, E.M.; Lafortune, M.A. Relationships between Ground Reaction Force and Tibial Bone Acceleration Parameters. *Int. J. Sport Biomech.* **1991**, *7*, 303–309. [[CrossRef](#)]
35. Butler, R.J.; Crowell, H.P.; Davis, I.M. Lower Extremity Stiffness: Implications for Performance and Injury. *Clin. Biomech.* **2003**, *18*, 511–517. [[CrossRef](#)] [[PubMed](#)]
36. Asaeda, M.; Deie, M.; Kono, Y.; Mikami, Y.; Kimura, H.; Adachi, N. The Relationship between Knee Muscle Strength and Knee Biomechanics during Running at 6 and 12 Months after Anterior Cruciate Ligament Reconstruction. *Asia-Pacific J. Sports Med. Arthrosc. Rehabil. Technol.* **2019**, *16*, 14–18. [[CrossRef](#)]
37. Strohrmann, C.; Harms, H.; Kappeler-setz, C.; Tröster, G. Monitoring Kinematic Changes with Fatigue in Running Using Body-Worn Sensors. *IEEE Trans. Inf. Technol. Biomed.* **2012**, *16*, 983–990. [[CrossRef](#)]
38. Cormack, S.J.; Mooney, M.G.; Morgan, W.; McGuigan, M.R. Influence of Neuromuscular Fatigue on Accelerometer Load in Elite Australian Football Players. *Int. J. Sports Physiol. Perform.* **2013**, *8*, 373–378. [[CrossRef](#)]
39. Buttfield, A.; Ball, K. The Practical Application of a Method of Analysing the Variability of Within-Step Accelerations Collected via Athlete Tracking Devices. *J. Sports Sci.* **2020**, *38*, 343–350. [[CrossRef](#)]

Disclaimer/Publisher’s Note: The statements, opinions and data contained in all publications are solely those of the individual author(s) and contributor(s) and not of MDPI and/or the editor(s). MDPI and/or the editor(s) disclaim responsibility for any injury to people or property resulting from any ideas, methods, instructions or products referred to in the content.